Optical Fiber and Preform Profiling Technology

W. J. STEWART

(Invited Paper)

Abstract—A comprehensive review of state-of-the-art optical fiber and preform index-profiling methods has been prepared. The advantages and disadvantages of the various approaches are discussed. Important parameters include measurement accuracy, resolution, simplicity, and the nondestructive features of some methods. Both optical and nonoptical techniques have been treated. Resolution considerations probably favor the refracted near-field technique and this may be a decisive factor for the measurement of single-mode fibers. Simplicity of apparatus lies with near-field methods generally so that the bound near-field method is most often used for dimensional measurements. Preform profiling is dominated by deflection function methods, usually accompanied by spatial filtering or focusing. Methods restricted to certain classes of fiber, such as the far-field approaches, are less attractive and, consequently, do not receive as much use.

Introduction

FOR both multimode and single-mode fibers the refractive index distribution of the core region, both axially and transversally, largely determines all important optical properties of the fiber other than attenuation. However, in fibers, it is not generally practicable to measure the axial variation of index distribution directly over any substantial part of the fiber's length, and fiber index profiling is therefore essentially a local measurement. For this and other reasons, the bandwidths of multimode fibers are generally measured independently. Bandwidth measurements, however, give little insight into the nature of any errors from the ideal profile. The use of differential mode delay (DMD) [1], on which an extensive literature now exists, improves this and gives some general profile error data, but the direct measurement of the profile still gives vital extra information. Also, the profiling of multimode preforms may enable poor examples to be rejected before drawing, and this has obvious economic benefits.

Profiling systems are also used to give essentially dimensional information such as core diameter and maximum index difference (NA) and, indeed, nearly all methods of assessing these are also useable to determine the profile. Such dimensional information is, however, used differently from profile shape data, for example, to determine splice or microbending loss, and this impacts upon the accuracy required. This review is concerned primarily with methods that give reasonably detailed profile shapes.

Manuscript received April 1, 1982. This work was supported in part by a British Telecom Contract.

The author is with the Allen Clark Research Centre, Plessey Research (Caswell) Limited, Caswell, Towcester, Northants., England.

The majority of methods considered are techniques for measuring actual refractive index, but methods for determining related quantities, such as composition, are also used. These are generally of less significance and will be considered at the end of this discussion.

The reader of the literature, especially the earlier literature, will find references to "destructive" and "nondestructive" techniques. This usually distinguishes between methods that are axial, requiring a flat end, or transverse, respectively. This distinction is of little practical significance for fibers, since virtually all methods require the removal of the primary coating and are therefore effectively destructive (nor is this really much of a disadvantage), but is of great significance for preforms where axial methods are therefore used primarily for reference.

One further general point; it may be a source of some surprise to many readers that relatively few workers are concerned with making profile measurements at wavelengths representative of those at which the fiber will be used, many measurements being made in the visible. The reason that this is acceptable is partly connected with the accuracy requirements discussed later. Its convenience is obvious, and the consequential improvement in spatial resolution is frequently valuable. Nevertheless, if the measurement is intended to yield an accurate value for numerical aperture, some consideration must be given to the variation with wavelength of this quantity. However, measurements show that this is quite small, NA varying by less than 1 percent over the wavelength range 600-1600 nm [2]. (Effects grow larger for wavelengths shorter than this.) Furthermore, in order to produce a variation in the profile shape of a multimode fiber with wavelength, such a change would have to be nonlinearly dependent on refractive index. Such an effect is not observed [2] in most fibers, and would almost certainly be too small to be perceived in such fibers by available profiling techniques. Certain special multidopant fibers could, however, show it. The reader should not confuse this *actual* variation of profile with wavelength with the well-known variation of *optimum* (multimode) profile with wavelength, a consequence of the dispersion in index, which is relatively large. Most of the profiling methods discussed can be used at any wavelength.

Accuracy requirements on profile index depend upon whether the fiber is monomode or multimode. For multimode it is frequently suggested that accuracy is required to a few parts in 10^5 (of the index) if satisfactory bandwidth predictions are to be made. This alarming figure is accurate,

0018-9480/82/1000-1439$00.75

but somewhat deceptive. In fact, measurements of absolute index are required, if at all, only for composition estimation and this is only rarely used. Measurements of peak index difference (Δ) are more generally required, and indeed many profiling methods only give difference information. The accuracy with which Δ is required is normally a few percent at most, but dispersion measurements are more demanding and special versions of the bound mode near-field [3] and axial interference [4] methods have been used for this purpose. Accuracy approaches 10^{-5} of the index.

In practice, the bandwidth of multimode fibers is influenced much more by changes of profile shape than by Δ, and the requirement is correspondingly for linearity and sensitivity at $1:10^5$ over a range of about $1:10^2$, rather than for absolute measurements. Most profiling methods can probably achieve this level of accuracy if performed sufficiently carefully, exceptions perhaps being those subject to unpredictable systematic shape errors such as bound near-field and reflectometry. For monomode fibers requirements may be looser except for special fibers such as "W" profiles; but since what is actually required is often an estimate of "V" value, it should be borne in mind that requirements for spatial accuracy may be twice as tight as those for index difference.

Spatial accuracy requirements are probably on the order of a percent or two of core radius for multimode fibers and (except as noted above) a few percent of radius for monomode. Again, however, linearity is required at much greater precision than this for multimode, say about 0.1 percent of radius. Extra resolution is always useful, but is particularly so for monomode fibers where it is necessary to achieve accuracy.

It is unfortunately true that no profiling method meets all the above requirements simultaneously with complete ease, and some compromise is therefore likely to be necessary. However, it is also true that in many cases the ultimate performance achieved is less significant than the ease with which fairly good performance can be obtained. A comparison on this basis is likely to be rather subjective, and this review does not attempt it, except in very general terms.

Various properties of optical fibers and, therefore, of the preforms from which they are made, are either essential or beneficial to most profiling methods. The most important of these are the small value of $\Delta(\lesssim 10^{-2})$ which can be relied upon except in the case of air inclusions, and the short-distance axial uniformity of the profile. This can be relied on over several core diameters in fibers because of the large draw-down factor from the preform ($\sim 10^4$) and the high viscosity during drawing. It is less reliable in preforms. Many transverse profiling methods initially assume circular symmetry, and most fibers and preforms are, of course, approximately circular symmetric. This may however cause inaccuracies even when the noncircularity is insignificant in itself and some monomode fibers may be deliberately made highly acircular to control their polarization properties. Most transverse profiling methods have been adapted to use computer tomographic techniques in order to cope with this, and these are considered later. Most axial profiling methods are unaffected by departures from circularity.

Many fibers will include index structure well below the resolution limit of any method, that is, between $\lambda/2$ and $\lambda/3$. This will not generally be true of collapsed preforms.

Individual Profiling Techniques

The following sections consider various particular profiling technologies. Because there are a large number of these and because many of them share features in common, they have been grouped initially according to whether they are axial, operating at least in part through an end face perpendicular to the axis, or transverse. They are grouped within this division according to their principles of operation since this allows certain considerations to be introduced at an appropriate stage. They are not grouped according to their suitability for use on fibers or preforms since many of them can be used for either. (Where appropriate, the preferred area of application is given.)

Nearly all widely used methods are included, as far as the author is aware, although the relative space devoted to each may perhaps reflect his prejudices and experience. The methods are not in any particular order, except as the grouping requires. Nonoptical methods are considered last.

A. Axial Profiling Techniques

These methods all require a flat perpendicular end on the fiber or preform. The tolerance on errors from perfection in this respect depends upon the technique used. In general it is possible to cleave an end on a fiber that is of sufficient quality, but for interference microscopy polishing must be used. Preforms must always be ground and polished to obtain the required end.

The resolution of all these methods will ultimately be limited by the collection angle of light from the fiber end, in the same way as for any other imaging system, but in many cases other effects will limit resolution more severely.

Microscopic Methods: The majority of axial profiling techniques involve the observation of the flat end with an imaging system, which in the case of fibers, for which this class of techniques is most significant, would be a microscope. The resolutions of all such methods are therefore limited by the objective NA, although again other effects may reduce this. High resolution systems will work better at relatively short wavelengths not only because this improves resolution directly, but also because the required imaging systems are not available at other wavelengths.

Any of these methods may be used either with the entire fiber end illuminated simultaneously and light passing from the object through the observing lens to an image (imaging microscopy) or with a beam passing in the opposite direction through the observing lens forming a small spot on the object which is then scanned to build up an image (scanning microscopy). The former method gives a multiplex advantage with an incoherent source and an imaging detector, but relies upon the imaging system for dimensional tolerances. The latter gives sensitivity advantages because of scattered light considerations and is less demanding upon the optics since it is usual to scan the object mechanically in front of a fixed focus. The former arrangement is preferred generally for interferometry and the latter for refracted near-field and reflectometry.

The Reflection Method: The principle of this method originally developed by Eickhoff and Weidel [5], and Ikeda, Tateda, and Yoshikiyo [6], [7] is shown in Fig. 1. A laser beam is focused onto the end of an optical fiber and the

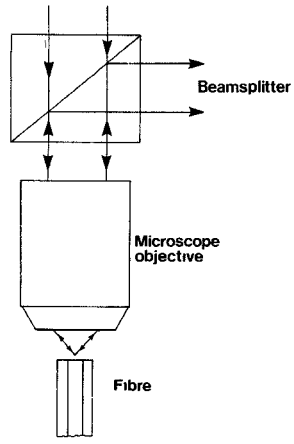

Fig. 1. A diagram of the basic apparatus used in reflectometric profiling.

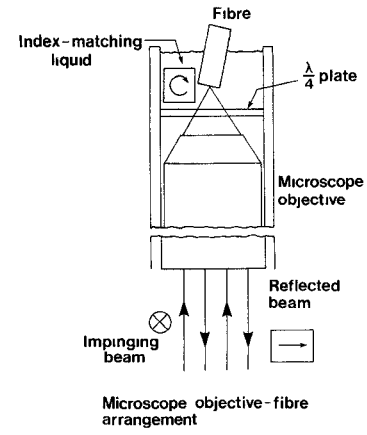

Fig. 2. The technique used by Calzavara, Costa, and Sordo [9] to improve signal-to-noise ratios in reflectometry.

reflectivity variation as the spot is scanned across the fiber end face is measured. The method is intuitively attractive and appears simple. However, both the variation of reflectivity with index for a typical fiber and the overall reflectivity are rather small, and these effects combine to give a system that is not very sensitive and rather prone to systematic errors. Eickhoff and Weidel [5] estimated the errors in Δ to be ± 0.0015, limited by noise and surface contamination effects. This also represented the sensitivity. The reflectivity change is usually analyzed as for a plane wave at normal incidence using the simple Fresnel equation

$$\text{reflectivity} = \left\{\frac{n_1 - n_2}{n_1 + n_2}\right\}^2 \tag{1}$$

where the indexes n_1 and n_2 are those of the fiber and the medium in front of the fiber face. According to this analysis, the change in reflectivity is very nearly linearly dependent on index change for small index changes. A more accurate analysis using the vector Fresnel equations for off-normal incidence supported this if air is the medium in contact with the fiber face [8].

In practice, a number of changes have been found necessary to improve the performance of this method. First, the use of linearly polarized light with a $\lambda/4$ plate can help suppress unwanted reflections [6], especially if it is located between the fiber end and the microscope objective, as was done by Calzavara, Costa, and Sordo [9]. Their arrangement is shown in Fig. 2. This system also uses an immersion oil around the fiber end. Although this decreases the absolute reflectivity, the relative reflectivity change across the fiber is considerably increased and the noise limited accuracy was improved to about 10^{-4}.

However, other problems remain, in particular, the relatively large effect of surface contamination. This may be understood if it is realized that a grading of refractive index between the immersion liquid and the fiber over about $\lambda/4$ ($\sim 0.2\ \mu$m) would suppress the reflection almost completely. It is therefore hardly surprising that a layer 300 Å thick can seriously affect the results, as was found by Stone and Earl [10]. They found that such a layer could be produced if the fiber end was polished rather than cleaved and could also form as a result of atmospheric attack. Although this effect is more pronounced with some dopants than others, it probably represents the principal reason for the relative unpopularity of this method.

The resolution actually obtained with this method is usually about 1 μm, it being generally assumed that it is similar to that of a normal microscope. It does not, however, seem to have been considered that the effect of immersing the fiber end is to reduce Brewster's angle to an NA of about 1.0. The combination of this with the polarization system used to suppress reflection may well prevent high resolution being obtained. The "type II" scanning optical microscope system [11] might be used to improve the resolution, but at the expense of optical efficiency in a system already notably poor in this respect.

The already-noted difficulty with polished faces means that this technique is only suitable for fibers, since preforms cannot be cleaved.

Near-Field Techniques: These comprise the most widely-used optical fiber profiling techniques, but are relatively little used with preforms. The following analysis of their principle of operation is different from those to be found in the literature and is used in order to show the similarity between the methods.

In all these methods, as described here, a small spot is focused upon a flat end face formed on the end of the fiber or preform that is perpendicular to its axis. The spatial information required is found by scanning the spot over the end face. However, the arguments given apply equally if the direction of light propagation is reversed and an image is formed of the end face. In both of these cases the light source will be effectively incoherent since in the scanned case no two points are illuminated simultaneously.

Consider Fig. 3, which represents a simplified picture of a cone of rays (or component plane waves) of semiangle θ, focused upon the end of a fiber of index n_2, surrounded by a medium of index n_3. The refractive index of the medium in front of the fiber face is n_1.

The usual form of Snell's law for the refraction between the media (n_2) and (n_3) would be

$$n_2 \cos\theta_2 = n_3 \cos\theta_3 \tag{2}$$

which may be rewritten as

$$k_{z2} = k_{z3} \tag{3}$$

where k_{zi} is the z component of the local k vector for the

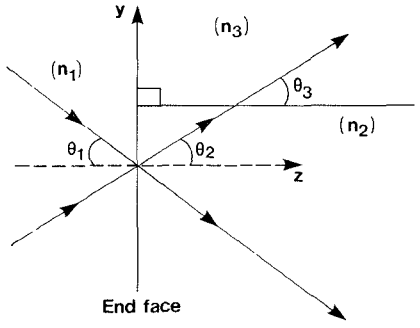

Fig. 3. A diagram of the fundamental process involved in near-field profiling. Areas to the right of the end face are within the fiber whose axis is horizontal.

wave in medium "*i*." This implies conservation of k_z through any media providing that all index structure is independent of z. As already noted, this condition is quite accurately met in fibers and approximately met in preforms.

The value of k_z to the right of the end face is therefore conserved, and it is determined by the refraction that occurs at the point of launch on the end face for which Snell's law can be written

$$k_{z1}^2 = n_1^2 k_o^2 - n_2^2 k_o^2 + k_{z2}^2 \tag{4}$$

where k_o is the free space k vector. Since k_o and n_1 are known, the value of k_{z2} corresponding to a given value of k_{z1} (or vice versa) uniquely determines n_2. This is the basis of the near-field profiling methods. In practice, however, it is not possible to measure k_{z1} and k_{z3} (or θ_1 and θ_3) directly in fibers because the resolution obtained would not be sufficient, although an equivalent measurement technique has been recently reported for preforms [12]. More commonly, a complete cone of rays up to some maximum value of θ_1 is launched. This will have a power distribution $P(k_{z1})$ and will produce a distribution $P(k_{z2})$ after refraction at the end face. If the former is known, measurement of the latter uniquely determines n_2 since the reflected light at the end face is negligible. In practice, however, such a complete measurement is unnecessary and inconvenient, and a simpler method is used. The distribution $P(k_{z2})$ is divided into two at some value of k_z, say k_{zf}, and the total of all light with either greater k_z or less k_z than k_{zf} is measured. Since the total launched power is known, these measurements are interchangeable and either will give sufficient information to reconstruct the profile.

In order to calculate the way in which the power detected after this division or filtering varies with n_2, use is now made of the fact that the expected fluctuations in n_2 are relatively small. It is also convenient to refer calculations to the region n_1. Using Snell's laws, as given above, the value θ_{1f} corresponding to k_{zf} is computed as

$$\cos^2 \theta_{1f} = 1 - \frac{n_2^2}{n_1^2} + \frac{k_{zf}^2}{k_o^2 n_1^2}. \tag{5}$$

Differentiating to find the rate of exchange of θ_{1f} with n_2, other things being constant, gives

$$2 \sin \theta_{1f} \cos \theta_{1f}\, d\theta_{1f} = \frac{2n_2}{n_1^2}\, dn_2. \tag{6}$$

The rate of change of detected power (P) with n_2 can now be computed if the launch distribution $P(\theta_1)$ is known, assuming azimuthal symmetry of this distribution. (It is more convenient to use $P(\theta_1)$ than $P(k_{z1})$, but these are equivalent.) This then gives

$$\frac{dP}{dn_2} = 2\pi \sin \theta_{1f}\, d\theta_{1f} \cdot P(\theta_{1f}) = \frac{2n_2}{n_1^2} \cdot \frac{\pi P(\theta_{1f})}{\cos \theta_{1f}}. \tag{7}$$

It is interesting to note that if $P(\theta_1)$ is proportional to $\cos \theta_1$, then the rate of change of power measured with n_2 is independent of θ_{1f} and, therefore, of k_{zf}. This is, of course, the distribution normally referred to as Lambertian, although this description really applies only to thermal (incoherent) sources. Note that even in this case the system is not linear in n_2 (being linear in n_2^2), but for the expected changes in n_2 this is a small effect. It is also fairly clear that (under the same conditions) the exact form of $P(\theta_1)$ is not crucial provided that it is nearly uniform and free from small-scale fluctuations with θ_1.

The foregoing description describes any of the near-field profiling techniques which differ mainly in the way in which the filter with its boundary at k_{zf} is implemented. In conventional, or bound near-field (BNF) profiling [13] the fiber's own numerical aperture is used. In an ideal fiber this is spatially invariant and passes all light of $k_{z2} > \beta_c$ (small θ_2), where β_c is the well-known cutoff propagation constant. This is, of course, fully true anywhere in a graded fiber core or in the cladding, but no light with $k_{z2} > k_{zf}$ is launched if n_2 is less than the cladding refractive index. In the refracted near-field (RNF) technique [14] the filter is a fixed physical aperture located in the constant refractive index medium n_3. It is usual in this case to measure the light with $k_{z2} < k_{zf}$ (large θ_3) because the other part of the distribution consists partly of guided and partly of radiation modes, but to measure this is also possible. The respective features of these methods are discussed in separate sections that follow.

Methods for obtaining accurate focus are important. For imaging methods, the focus can be optimized easily. For scanning methods, either the system may be operated backwards in an imaging mode for setup or, more effectively, the scan can be made fast enough to be displayed in real time on an oscilloscope (as for Fig. 13). The high optical efficiency makes this possible and at the highest resolutions it probably constitutes the only way of setting up accurately.

Resolution of Near-Field Techniques: The unified description of near-field methods just given will now be used to show their spatial resolution properties. Again the discussion will assume that light is being launched into the fiber, but the results apply also if the optical propagation direction is reversed. The discussion will refer to numerical apertures (NA's) or angles rather than k_z values because this is more easily related to the usual optical resolution calculations, it being understood that these are measured in the medium of constant refractive index n_1 in which an exact correspondence with k_z exists

$$k_z = n_1 k_o \cos \theta = k_o \sqrt{n_1^2 - (\mathrm{NA})^2}. \tag{8}$$

Let the NA of the edge of the launched beam be N_1 and the NA within the launch beam corresponding to the filter edge be N_2, so that

$$N_2 \equiv n_1 \sin(\theta_{1f}). \tag{9}$$

Two different physical mechanisms limit the resolution according to whether N_2 is small compared to N_1, or N_2 approaches N_1. These will first be considered separately and a unifying description will then be given. We take the latter case (N_2-N_1) first. In Fig. 4 an input beam is focused and the far field observed. Although it is usual to consider the distortion of the near field due to partial obstruction of the far field, this effect will equally occur the other way around and the beam profile in the far field will be distorted by the presence in the focal plane of an object of limited extent as illustrated. It is obvious that the power change due to an index change in near-field profiling will alter if the distortion is significant at N_2, and that this effect will therefore increase as N_2 approaches N_1. It would be possible to compute this effect directly, but it is simpler to note that it will occur equally with absorbing objects and is therefore closely similar to the effect observed in a microscope with an annular aperture extending from N_2 to N_1, and can be calculated in the same way [15].

The result of this calculation showing the resolution "s" as a function of N_2 for $N_1 = 0.5$ is shown in Fig. 5 labeled "annular lens N_1/N_2." As might be expected the resolution is affected strongly only as N_2 closely approaches N_1.

The other mechanism, as N_2 becomes small, is peculiar to near-field profiling. In order to simplify the analysis a two-dimensional case is considered in a single y-z plane. In Fig. 6 a situation somewhat similar to that in Fig. 3 is illustrated, except that a Fresnel reflected wave "2" is included. It is reasonably clear that the rays "1" and "2" will interfere to produce a resultant intensity $P(k_z)$ that is oscillatory as the point of launch to interface distance y is varied. Ray 3 is of course constant, so this oscillation as the spot is scanned will show up in the measurement. If the rays are integrated from N_2 to N_1 with this effect included, the results shown in Fig. 7 are obtained, all for $N_1 = 1.3$. The curves also include the step expected from the index changes indicated, which are assumed to be sharp. The curves are normalized to the same step height. This simple theory is expected to fail if the spot overlaps the interface as it will between the dotted lines, the range of which is illustrated by the line spread function shown at the bottom. The curves are interpolated in this region. It can be seen that the effect of the accumulated Fresnel reflections is to reduce the resolution in much the same way as observation with a lens of NA = N_2 would have done, but not to the same degree. This effect is largely independent of $\Delta n = n_3 - n_2$ as illustrated.

After the discussion of reflection techniques the reader may feel that Fresnel reflection is an effect that could be eliminated, but this is not so in this case. If the index step were graded enough to prevent reflection (the degree necessary is illustrated in Fig. 7 labeled "Fresnel") then the "resolution" is irrelevant. The reader may easily verify that the same is true of an antireflection layer. The curve for the resolution of a simple lens of NA = N_2 is therefore illustrated in Fig. 5.

It is expected in practice that the resolution will show some transition between these two effects for intermediate N_2.

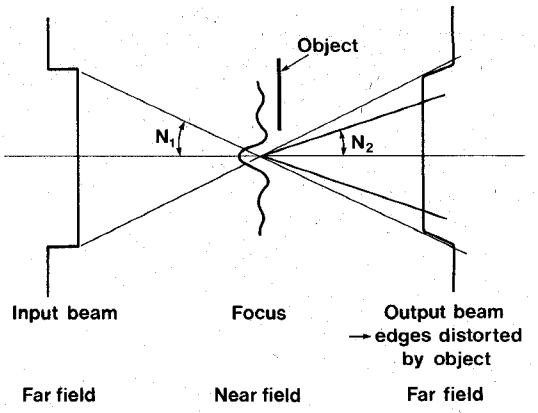

Fig. 4. A diagram illustrating the mechanism for declining resolution at high N_2 in near-field methods.

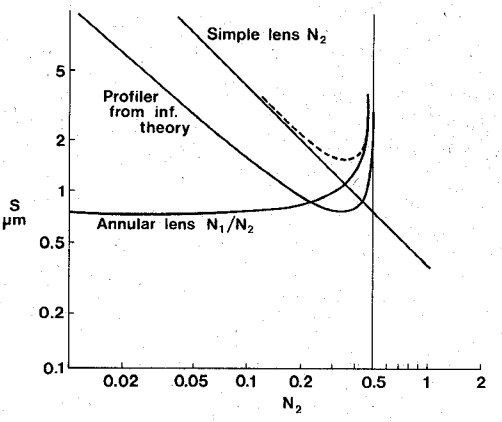

Fig. 5. A theoretical calculation of resolution in μm ($\lambda = 633$ nm) against angular filter NA, for near-field profiling methods.

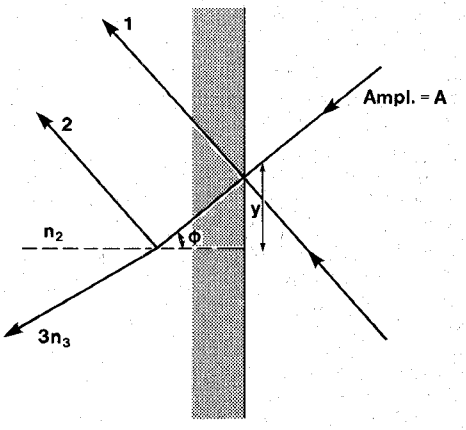

Fig. 6. Illustrating the mechanism for loss of resolution at small N_2 in near-field profiling methods.

This effect is illustrated in Fig. 8 which shows results using refracted near field. The resolution, measured as 20-80 percent rise distance is actually, however, better than might be expected.

To cover the general case, the following analysis based upon the information content of the beams has been devised [16].

Consider a light beam of NA = N passing through a circular aperture of radius "a." By considering the finest fringes that can be produced and by using the Nyquist rate, the number

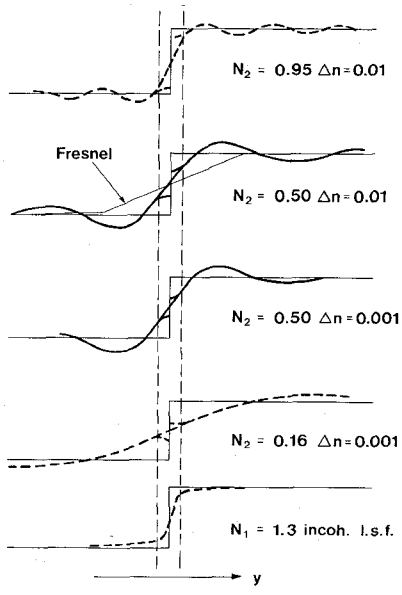

Fig. 7. Results of a calculation of edge response limited by the small N_2 mechanism for near-field profiling techniques. The curve labeled "Fresnel" shows the index gradient necessary to suppress reflection.

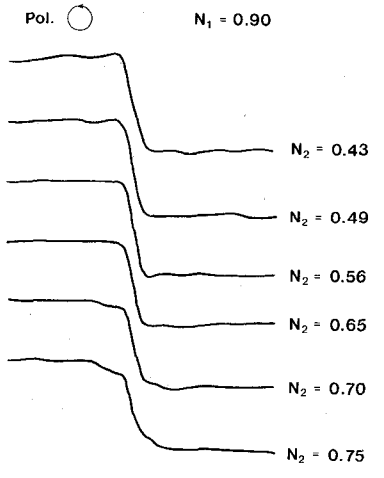

Fig. 8. Actual traces of the response of an RNF profiler to a sharp index step showing the changing response and the optimum N_2.

"m" of discrete beams that could be passed through the aperture (i.e., the number of degrees of freedom) can be shown to be

$$m = \frac{4\pi N^2}{\lambda^2} a^2 \tag{10}$$

where λ is the optical wavelength. If this is inverted to produce the area for a single degree of freedom, and if it is assumed that such areas could be hexagonally close packed, their separation is given as

$$0.606 \frac{\lambda}{N}$$

compared to the Rayleigh criterion of $0.61\ \lambda/N$. This description is equally successful with annular apertures, but the profiler requires a more elaborate treatment. Let the number of degrees of freedom associated with N_1 and N_2 be m_1 and m_2, respectively. The profiler divides the group m_1 into two groups m_2 and $(m_1 - m_2)$, in a way dependent upon n_2. The information carried by this division is assumed to be given by the number of different ways in which it could be made, which is well known to be

$$\binom{m_1}{m_2} = \frac{m_1!}{m_2!(m_1 - m_2)!}. \tag{11}$$

The number of binary bits that this represents is then

$$\log_2 \binom{m_1}{m_2} = \frac{1}{\log_e 2} \{m_1 \log_e m_1 - m_2 \log_e m_2 - (m_1 - m_2) \cdot \log_e (m_1 - m_2)\} \tag{12}$$

if m_1, m_2 are large.

Partial division of a degree of freedom between m_2 and $(m_1 - m_2)$ can be coped with by dividing each degree of freedom into 2P fractions and also dividing the answer into p-levels, giving the same result.

Having derived m_1 and m_2 using (10) the number of binary bits given by (12) is reused in (10) in place of m and the equation again inverted to give a spatial area per bit. Again assuming hexagonal close packing, a resolution is derived. The resulting expression is

$$\text{Resln} = \frac{1}{N_1} \left[- \frac{2\lambda_0^2 \log_e 2}{\pi\sqrt{3}(f \log_e f + (1-f) \log_e (1-f))} \right]^{1/2} \tag{13}$$

where

$$f \equiv \left[\frac{N_2}{N_1}\right]^2.$$

The calculated result is shown in Fig. 5 labeled "profiler from inf theory." As might be expected it shows maximum resolution when $m_2 = (m_1 - m_2)$ or

$$N_2 = \frac{N_1}{\sqrt{2}}. \tag{14}$$

This does give a fairly accurate picture for small N_1, N_2, but at larger values an additional effect occurs because the angle of convergence of the rays at the edge of N_1 approaches 90°. For one polarization the fringe contrast produced then falls to zero. This results in a smaller optimum N_2 because the effective number of degrees of freedom near the edge of N_1 is reduced. Fig. 9 shows the result if this effect is included. Fig. 10 shows some experimental results (from RNF since in BNF the values of N_2 are hard to obtain) for comparison. Although there are some differences in the values, as might be expected, the general behavior is well explained. The effect of changing polarization is discussed with RNF later since it is of little significance for BNF.

The Bound Near-Field Technique (BNF): This was originally developed by Sladen, Payne, and Adams [13] in the "reversed" form (compared to the above descriptions) in which light launched into a fiber is observed with a microscope as it emerges from the end face. The apparatus used is diagrammed in Fig. 11. The scanning version was later developed by Arnaud and Derosier [17]. Either method may be used according to convenience.

As explained above, in BNF, the filter with its boundary at

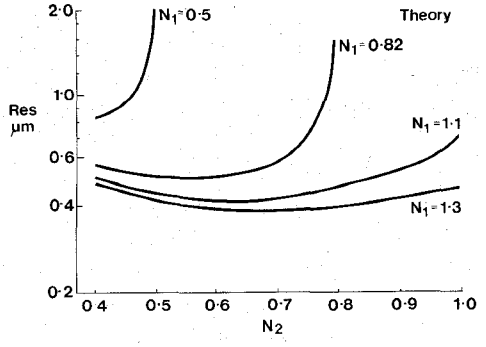

Fig. 9. Theoretical response calculated on the information content argument for RNF (and BNF). Curves are of resolution (633 nm) versus filter NA(N_2) with objective NA(N_1) as a parameter.

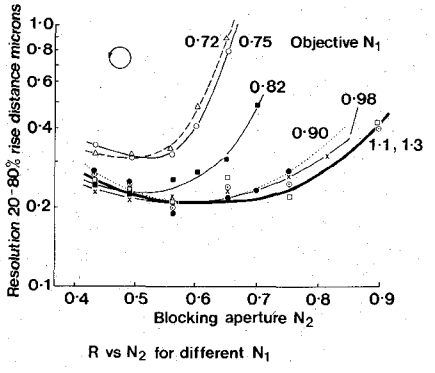

Fig. 10. Experimental curves for comparison with Fig. 9.

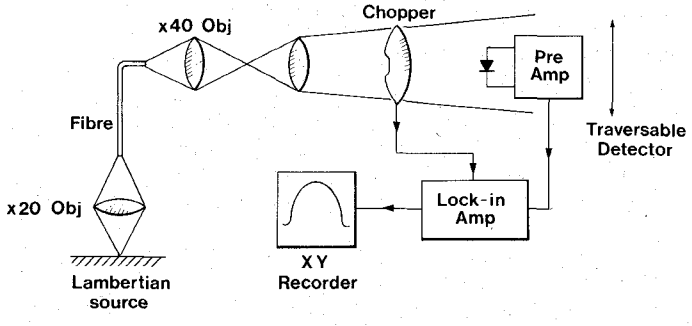

Fig. 11. Outline of the apparatus used by Sladen, Payne, and Adams to perform BNF [13].

k_{zf} consists of the fiber's own numerical aperture, so that

$$k_{zf} = k_0 n_c$$

where n_c = cladding index.

This has advantages and disadvantages. The greatest advantage is that it keeps the apparatus very simple since no physical filter is required. A secondary advantage is that, for the same reason, no misalignment between the fiber axis and the filter axis, such as can occur in RNF, is possible. The disadvantages are relatively poor resolution, especially near the edge of the core [18], [19] data only where $n > n_c$ (i.e., in the core) and the leaky mode problem. The loss of resolution is particularly acute for small fiber NA's, and an attempt to profile single-mode fibers simply produces the mode shape. BNF is not, therefore, usable with monomode fibers.

The leaky mode effect is perhaps more serious. It was mentioned earlier that the filter must be spatially invariant. Unfortunately, the presence in circular cross section fibers of leaky modes [20] means that this condition is effectively not met. The presence of these relatively low-loss unguided modes means that the cutoff k_{zf} is smaller near the edge of the core where they are more abundant and is also length-dependent. They remain significant for any practical measurement length and, in general terms, cause the index near the edge of the fiber core to appear substantially greater than it actually is. For the ideal circular fiber this effect can be corrected for using an ingenious radius-dependent correction factor due to Adams, Payne, and Sladen [21] which is normalized for length using the parameter

$$\frac{1}{V} \log_e \left(\frac{z}{a}\right)$$

where V has its usual meaning, z is the length, and "a" is the core radius. However, some workers have found that the correction factor can vary quite considerably from the ideal. The reason for this is probably connected with the near-degeneracy of different azimuthal modes in the fibers of most interest, which have near-parabolic profiles. This causes different azimuthal modes to be easily coupled by small departures from circular symmetry. Leaky azimuthal modes then lose power to radiation modes of similar propagation constant, reducing the correction required. This effect was first described by Petermann [22].

The BNF technique is still widely used in spite of these problems because of its simplicity, but is restricted to obtaining largely dimensional data and qualitative profile information.

There remains one "BNF" technique that circumvents some of the above difficulties. It is due to Sabine, Donaghy, and Irving [23] and takes advantage of the fact that some fibers are coated with low index plastic. This forms a larger step-index "fiber" with the whole original silica fiber as "core." The technique is now to perform BNF just as above on this "fiber." Note that k_{zf} is decreased because the NA is greater than that of the original fiber. The same problems with leaky modes may arise, but these are less if the actual fiber core is relatively small, and the original cladding is, of course, now profiled. This method is, however, of limited application and does not seem to be widely used.

The Refracted Near-Field Technique (RNF): This method was devised by Stewart [14] with subsequent development by White [15]. It is usual to use the scanning microscopy approach with RNF. The apparatus used by White is shown in Fig. 12. The role of the filter at k_{zf} is now taken by the disc below the liquid cell and the light not intercepted by this disc is measured.

The main advantages of this approach compared to BNF are greatly improved resolution, profiling of the whole fiber, and freedom from any leaky mode effects (under conditions discussed below). The main disadvantages are relatively increased sensitivity to dust and some increase in the complexity of the apparatus. The improved resolution is a consequence of the use of an increased N_2 as discussed above and is most useful for single-mode fibers, an example of which is shown

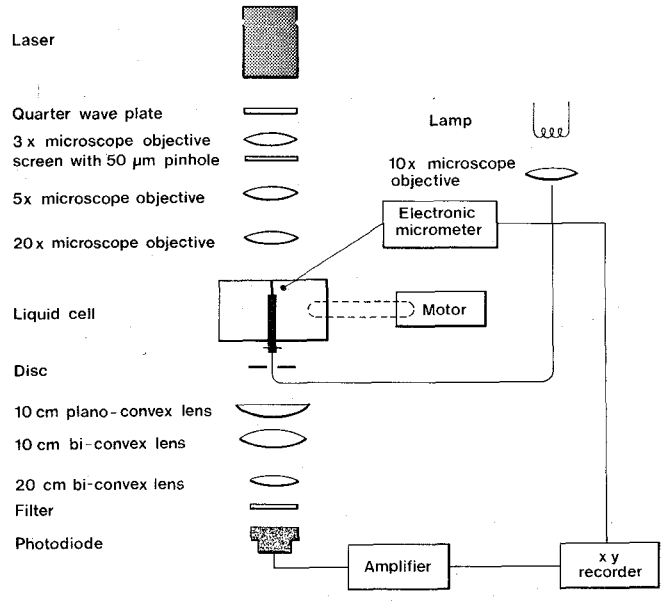

Fig. 12. The apparatus used by White [15] for RNF profiling.

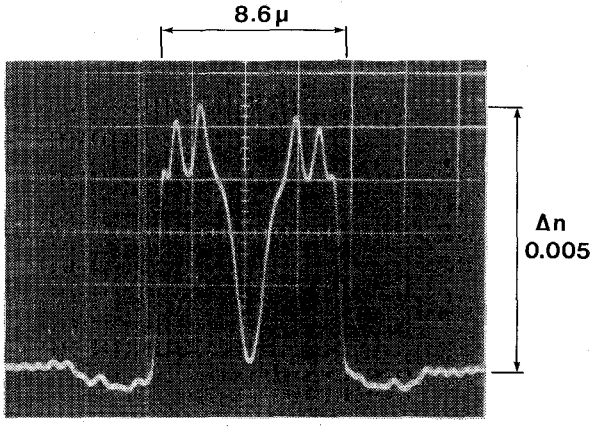

Fig. 13. A single-mode fiber measured by high resolution RNF. The trace is measured in real time at about 5 scans/s; it is also noise-free. The ripples are cladding layers.

in Fig. 13 for $N_1 = 1.1$ and $N_2 = 0.6$. Even layer structure in the cladding is resolved.

The original reason for deriving this method was, however, to eliminate the leaky mode effects found in BNF. This is possible because, for anything other than a pure step-index fiber, the range of propagation constants over which leaky modes occur is limited. If k_{zf} is set outside this range, then the effect of leaky modes is eliminated, since they are excluded whether radiative or not. The value of k_{zf} (and hence, N_2), necessary to achieve this, depends upon profile.

For the case of a parabolic profile, White [15] has shown that an $N_2 = 0.25$ is sufficient if the fiber's NA = 0.2. In practice, not only is this easily achieved, but any slight failure to achieve it produces little effect because the number of leaky modes always declines rapidly as N_2 increases.

The increased sensitivity to dust on the end face compared with BNF can be seen from (7), under which it was pointed out that the signal dP associated with a change in index dn_2 was independent of N_2 for a given $P(\theta)$. The relative change of measured power dP/P, therefore, declines with increasing N_2 because P increases [for a given $P(\theta)$] assuming that N_1 is increased in proportion with N_2. This effect is worthy of note, but in practice does not present major problems.

The effect of tilts in refracted near-field profiling has not been examined in detail in the literature, largely because it does not normally present problems, but it seems desirable to consider it here.

The origin of these effects can be understood quite simply by considering that all the arguments applied earlier to show that k_z is conserved equally show that k_y and k_x are not, although of course $(k_x^2 + k_y^2)$ must be. k_y and k_x are conserved only if the spot is launched on axis. It is therefore essential that the k_z filter (stop) should not be sensitive to changes in k_y or k_x, that is, that it should be accurately set in line with the fiber's axis. The effect produced if it is not will depend upon the detailed experimental characteristics. To understand this consider Fig. 14. On the left is a conventional illustration of an RNF profiler focused off the fiber core. To the right is an end-on view of the same situation. It can be seen that if, as is usual, the cell liquid's index is higher than that of the fiber, the latter acts as a negative lens. Below is illustrated the effect of this in k space—which coincides physically with the plane of the blocking aperture. The conservation of k_z means that any part of the launched light is confined to a circle on this diagram, but the effect of the fiber in the situation given above is to move light around the circle as shown, so that the distribution is no longer even in azimuth. This effect may easily be observed in an RNF system, and can be used to help locate the fiber. Of course if the filter (aperture) is centrally located, this will not affect the results, but if the aperture is high or low in y, (i.e., with a center at $x = 0$, $y \neq 0$), then the measurement will be high or low, respectively. The magnitude of this effect depends in a complex way on the cell liquid index, the fiber index, and for multimode fibers, the index profile. It can, however, be readily seen that the reading of "index" will differ according to whether the scan spot is above or below the fiber, and that the profile reading on axis is unaffected. In practice, the effect appears as though the whole profile (including the cladding index) were "tilted" and there is no danger that this will be confused with an actual index effect. It is, however, obvious from the above explanation that this is not an exact linear tilt and it should not be corrected electronically. If it is due to a tilt of the fiber within the cell (unlikely) or an error in the stop position it can be exactly corrected by transverse movement of the stop. Note that these errors are equivalent because a tilt of the input objective produces none of the effects described above. This effect is small, but there is no change with tilt of the input beam only if the distribution $P(\theta)$ is uniform. In this case only the edges of the distribution are affected and these are all detected anyway. If the fiber end is not perpendicular to its axis, see Fig. 15, a prism of liquid is formed between the end and the cell window. This will produce a similar effect to the tilting of the input beam, but the equivalent tilt may be a function of position on the end face because of the changing index of the fiber. As pointed out above, this effect is avoided if $P(\theta)$ is uniform,

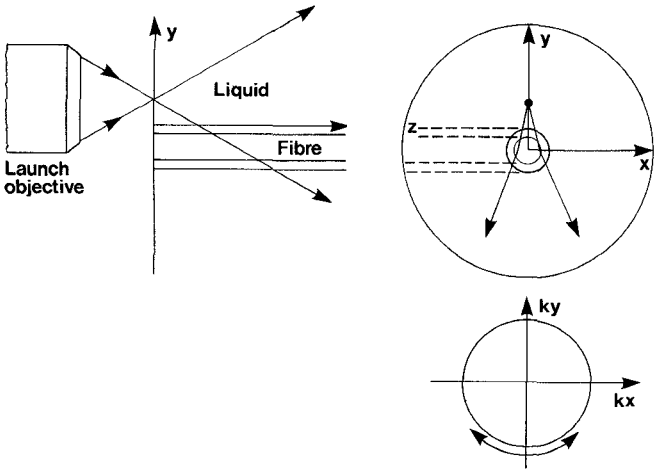

Fig. 14. Showing effects connected with stop position tolerances in RNF.

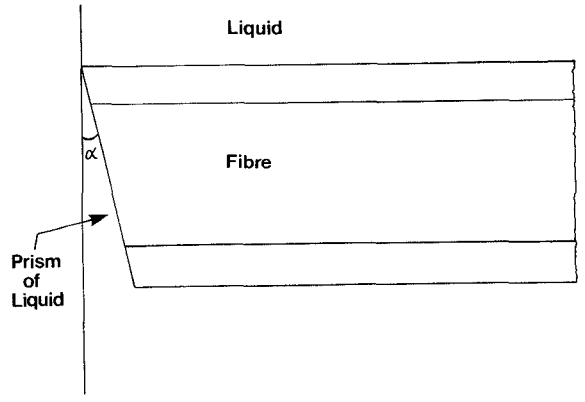

Fig. 15. The prismatic effect of a tilted fiber end.

although there is a residual asymmetric resolution effect that is rather small. In practice, an end that is tilted may not be uniformly so and it is best to use only ends of good quality. For the minimization of all these errors it is obviously desirable to keep the cell liquid index fairly close to that of the fiber, say between the core and cladding indexes. A tolerance on the end face angle is hard to give because of the dependence on other parameters, but an error of $<1.5°$ has been found satisfactory. In practice, it does not cause problems if the precautions above are taken.

At high N_1 the main effect of an end face tilt is likely to be due to defocus if the scan is linear. This effect is much the same as it would be in a conventional microscope.

Some effort has been devoted to calibration techniques for RNF. Young [25] has used a range of index matching oils with a single fiber. Saunders [24] used the differential index change with temperature between the cell liquid and the fiber. White [15] observed that if the value of N_2 is adjusted as the index n_2 is changed, in such a way as to keep the detected power constant, the effects of $P(\theta)$ are eliminated. This can be accomplished by moving the stop along the z axis, and the degree of movement required provides a relatively absolute measurement.

For high resolution measurements there are some further considerations. First, the high N_1 makes the collection optics difficult. This problem can be solved as in [26] by forming the walls of the liquid cell into an ellipsoidal mirror. The resulting apparatus is shown in Fig. 16. It is of some importance that the mirror reflectivity be uniform with angle or this will produce a more complex k_z "filter" than is required with possibly unfortunate results. Of course such a filter might be deliberately formed ("apodizing") to affect the resolution response, but this does not seem to have been tried. At these apertures the effects of polarization, although just on resolution, can be large, see Fig. 17, and circularly polarized light is used to remove them.

Although RNF is used primarily with fibers, there have been two recent applications to preforms. One, due to Okoshi and Era [27] is similar to the usual scanning version except that the central part rather than the outer part of the launched light is measured, that is the part with $k_z > k_{zf}$. As pointed out above, this is equivalent, but has some advantages because of the reduced aperture of the collection optics. It does, however, require that both ends of the preform are polished.

The other preform "RNF" method is due to Sasaki, Payne, and Adams [12]. It is classified with RNF because the optical path is similar, but it actually measures the refracted angle θ_1 directly and does not use the k_z filter. As with the other preform approach, it does require that a good quality end is produced on the preform and this may be a disadvantage.

Far-Field Profiling Techniques: These methods involve the measurement of the far-field exit-radiation pattern from a fiber; see Fig. 18. They have as their general advantage that there are no external optics to affect the measurement. They do, however, require a good quality fiber end.

The first method is appropriate only for multimode fibers and was suggested by Grau and Leminger [28] and first tried by Freude [29]. The method uses geometrical relationships between near and far fields and currently assumes circular symmetry, although this is not, perhaps, essential. As with some transverse methods errors tend to build up near the fiber axis and resolution is rather poor, perhaps a few microns. The method requires that the launched power distribution in the fiber is Lambertian. It would be prone to the effects of leaky modes, but it is claimed that these can be adequately stripped [29]. The method could be regarded as an alternative to BNF.

The other far-field profiling technique, called the exit-radiation method, is conversely applicable only to monomode fibers and is due to Hotate and Okoshi [30]. The apparatus and measurement method are similar, but a much wider range of angles θ is covered ($\pm 60°$) and the detector dynamic range required is correspondingly large (90 dB).

There are, of course, no problems with leaky modes or launch distributions, but the fiber must be monomode at the wavelength of measurement. The profile is obtained from the measurements using inverse Hankel transforms which are evaluated numerically on a computer. The resolution is good, being about $\lambda/2$ at the wavelength used. This method has not found wide favor, however, probably because of concern at the possible effects of dust and other extraneous light scattering in conjunction with the very wide dynamic range required. The reported method assumed circular symmetry, but this is

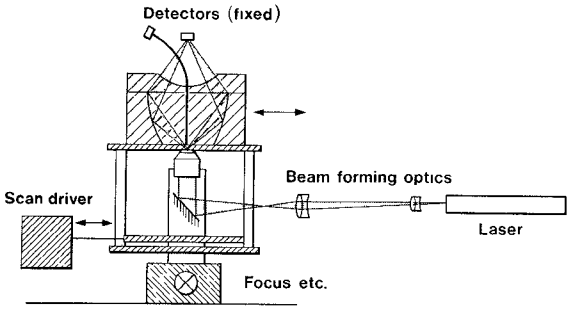

Fig. 16. The apparatus used by Reid and Stewart [26] for ultra-high resolution RNF profiling.

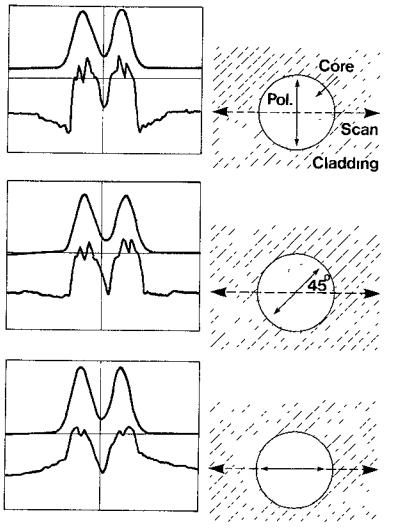

Fig. 17. RNF traces (lower trace in each case, upper is BNF) showing the effect of polarization direction with respect to scan direction. This relationship is indicated in the diagrams on the right.

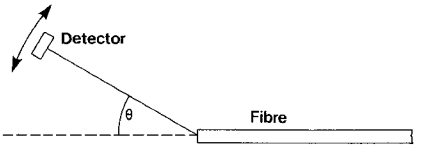

Fig. 18. Apparatus for far-field profiling.

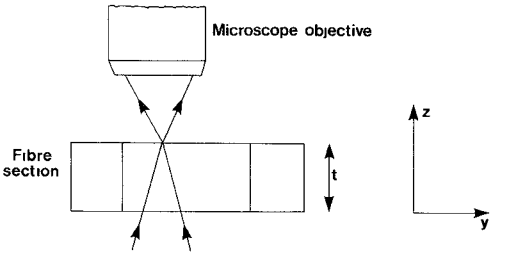

Fig. 19. Apparatus for axial interferometry.

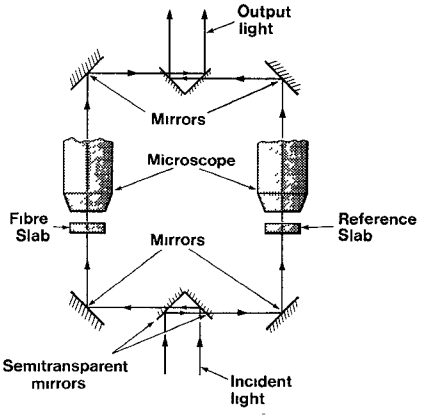

Fig. 20. Principle of operation of dual-beam interference microscope. From Marcuse and Presby [86].

Fig. 21. An example of the image obtained by axial interferometry with a graded multimode fiber. From Presby and Astle [34].

probably not essential, although a departure from circular symmetry would render the method more complex.

A reduced version of this method, reported earlier by Gambling, Payne, Matsumura, and Dyott [31] measured only the central part of the far field and gave only core diameter information.

Axial Interferometry: In this method a thin slice (thickness "t") is cut from a fiber or preform (see Fig. 19) and this is placed in a two-beam interference microscope (Fig. 20). The fringes observed can be related directly to the sample's optical thickness and hence, its refractive index as a function of transverse position. An example of the observed image is shown in Fig. 21. The method has been used by a number of workers [4], [32] and is applicable to both fibers and preforms. Its principal advantage is its absolute accuracy. Its principal disadvantages are the cost and complexity of the apparatus required, the care needed to prepare satisfactory samples, and (for fibers) its relatively poor resolution. The absolute accuracy of the method is inherent in all interferometric techniques, but in order to achieve it, some care is necessary in sample preparation [33]. For maximum accuracy the thickest possible sample is also desirable since this increases the number of fringes for a given index change. However, this also leads to significant ray bending within the sample and a compromise must be reached. A sample thickness of 100 μm would be typical for a fiber. Greater thicknesses can be used with most preforms. In order to maintain accuracy very small relative fringe shifts must now be measured (the total shift being only a few fringes) and electronic means are normally used to achieve this. Presby and Astle [34] used a video camera for this purpose, and measurements of 10^{-3} of a fringe precision could then be achieved. The relatively poor resolution is also a sample-thickness effect due to the

cone angle of illumination and/or ray bending effects, as a result of which the resolution is poorer than that of a conventional microscope with the same NA. This effect is well-known in interference microscopy. There is also a potential fringe ambiguity problem at sharp index steps, but this is not often important.

The complexity of the apparatus can be reduced by sandwiching the sample between partially transmitting mirrors and observing the resulting Fabry-Perot fringes [35] in a conventional (normally metallurgical) microscope.

In common with the near-field methods this technique can cope easily with noncircular fibers and preforms. The main reason for its relatively restricted use is probably the difficulty of sample preparation. In the case of preforms it is also, of course, destructive. It still, however, finds favor as a reference method.

It is also possible to use shearing interference axially [36], but this would be appropriate only with preforms where the thicknesses can be greater.

B. Transverse Methods

In transverse profiling methods an optical wave is passed transversely through the fiber or preform, usually immersed in a liquid, as shown in Fig. 22. Any single wavefront, for example, the one shown in the figure, suffers distortion as a result of differential phase delays caused by the varying refractive index. The resulting distorted wavefront (see Fig. 22) therefore contains information that can be used to reconstruct the index profile. In describing individual methods a distinction is drawn between those that observe the phase delay as a function of position and those that similarly observe the tilt of the wavefront or the ray bending. This is convenient, but the reader will be aware that this distinction is not very fundamental.

These transverse methods have many common features. They are nondestructive, although this is only really important for preforms. They tend to be less accurate close to the fiber axis for the simple reason that, in a circular symmetric fiber, very little axial material is traversed by the transverse illumination. The practical magnitude of this effect, however, depends a good deal on the actual method. They have high ultimate resolution because of the possible 360° range of illumination directions, although not all methods realize this in practice. Finally, they generally must resort to computer tomographic (CAT) techniques to cope with noncircular cross sections. These tomographic techniques will be considered later.

In many cases, however, it is possible to assume circular symmetry. In this case it can be shown that the phase shift as a function of y, $\psi(y)$ (Fig. 22) can be used to find the refractive index using the relation [37]

$$n(r) - n_2 = -\frac{1}{\pi}\int_r^\infty \frac{d\psi}{dy}\cdot\frac{1}{(y^2 - r^2)^{1/2}}\,dy \qquad (15)$$

where n_2 is the refractive index of the surrounding medium. This relationship is a version of the Abel transform, other versions of which may include a Bessel function. It is characteristic of cylindrical symmetry. This relationship is used with

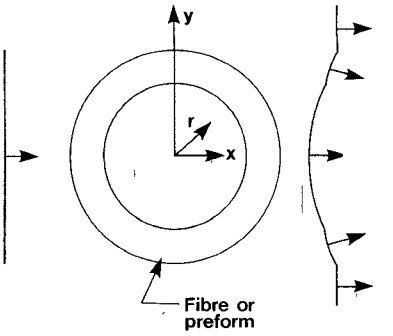

Fig. 22. The basis for transverse profiling. The effect on a wavefront of traversing an optical fiber or preform.

most transverse profiling methods. It is not exact because it ignores ray bending within the fiber or preform, but this is a small error in most practical cases. It is interesting to note that ψ enters only as $d\psi/dy$, that is, as the tilt of the wavefronts or the refraction angle of a ray. This same relation is therefore used with ray deflection methods with the tangent of the ray deflection angle replacing $d\psi/dy$. Another interesting feature is the way in which the index is obtained by integrating effectively from the outside (large y) inward, since only at large y is the index known. Each point nearer to the axis (smaller y) involves integrating over more (potentially inaccurate) experimental points. The increased errors near the axis for which a physical explanation was given enter in this way. This effect does not occur in the equivalent tomographic methods.

Various methods can be used to evaluate (numerically) the integral in (15). If the measured quantity is ψ some problems can arise and these are discussed in [37].

Transverse Interferometry (2-Beam): This is the transverse equivalent of the axial 2-beam interferometry technique discussed earlier and is normally applied only to fibers. This is because the rapid index fluctuations in and large thicknesses of most preforms cause measurement difficulties. However, by the use of spatial filtering and by exploiting some of their special properties, Okoshi and Nishimura [38] have succeeded in applying this approach to VAD preforms. Transverse shearing interferometry is used with preforms, but this is a deflection function method and is considered later.

Except that the sample is viewed transversely and is immersed in an index matching fluid, the experimental approach here is closely similar to that employed in axial interferometry as discussed earlier. An example of the image obtained is shown in Fig. 23. Of course the problems with polishing ends are avoided. Resolution is superior to that achieved with axial interference, partly because of the more favorable geometry, especially near the fiber axis, and partly because of the reduced effective sample thickness. Use can be made of the known axial invariance over short distances to improve fringe measurement errors. The method also has the advantage, in common with other transverse methods, that it can be used to measure axial changes in fiber profiles [39]. The method is probably less accurate than axial interference because of the reduced sample thickness, especially near the axis. It has received a good deal of attention over the years [38]-[46], but is not as widely used as other methods perhaps because of

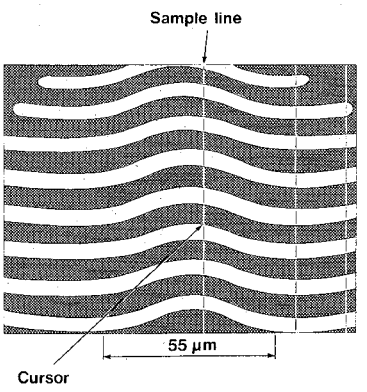

Fig. 23. An example of the image obtained by transverse interferometry with a graded multimode fiber. From Marcuse and Presby [86].

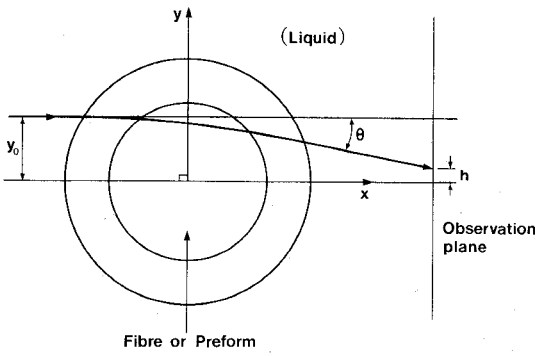

Fig. 24. Same for Fig. 22, but showing the ray deflection θ.

the complexity and cost of the apparatus required. The measurement of $\psi(y)$ is used in (15) to find the profile and this requires a computer. Some care is required to prevent errors building up during computation [37].

Light Scattering Methods: If the incident wave in Fig. 22 is coherent, then an examination of the scattered wave diffraction pattern will yield information on the profile. This is true whether the fiber is immersed in index fluid or not, although the former case is generally easier to handle. First attempts to use this with graded fibers [47] calculated the backscattered pattern from an air-spaced fiber and compared this with experiment. The system was run the other way, i.e., to deduce profile from scatter, by Okoshi and Hotate [48], [49] who used an immersion liquid. Use was made of the reflection from the cladding-liquid interface to provide a phase reference. Resolution was excellent, $\sim\lambda/4$, but the amount of computation involved is rather impressive, and this is probably why the method has not been widely used. A reduced method was devised by Saekeang and Chu [50] for air-spaced fibers.

A related method has been devised and developed by Brinkmeyer [51], [52]. This does not involve computation and uses an immersed fiber. Effectively, the transform in (15) is performed optically using a special optical system involving a spatial filter. The method could be extended to noncircular fibers using holographic techniques.

Deflection Function Methods: These methods all involve the measurement of the refraction of an incident ray as a function of transverse position of incidence y (Fig. 22). As already pointed out, this is equivalent to a measurement of $d\psi/dy$ as a function of y (15) to an adequate approximation. Many methods are more or less direct, but two, the focusing method and shearing interferometry, are slightly less so. These methods constitute by far the most popular approach to preform profiling where their nondestructive nature is important. They are less used with fibers probably because of their relatively modest spatial resolution.

If Fig. 22 is redrawn showing rays rather than wavefronts, Fig. 24 is obtained. The required deflection function is tan $\{\theta(y_o)\}$ or equivalently $h(y_o)$ if x is known.

Beam Deflection Techniques: The most obvious method of measuring $\theta(y_o)$ is to project a laser beam through the preform at a distance y_o from the axis and measure the deflection angle. This method was first used by Chu [53] and was subsequently developed by him and others [54]-[56]. To obtain better resolution it is desirable to focus the beam within the preform, but even so the resolution is poor (20-40 μm) and the method is only suitable for preforms. Its advantage would be the simplicity of the apparatus, but in this respect, it is not notably superior to other methods and it is probably no longer widely used. It is of interest as the earliest technique for measuring $\theta(y_o)$.

Deflection Function Imaging Methods: It has been noted that the deflection function can be observed directly by viewing an angled line through a fiber preform [57]. More sophisticated versions of this approach involve using a combination of cylindrical and spherical lenses to produce a display in which the deflection angle is "plotted" optically against position y [58], [59]. This image can then be analyzed to give $\theta(y_o)$ quite easily. In one realization due to Okoshi and Nishimura [58] and in a slightly different form to Sasaki, Payne, and Adams [60], a cylindrical lens [61] is used to image the preform in the y dimension (Fig. 25). Okoshi and Nishimura used a slit and a spherical lens. The other dimension is not imaged, but the triangular mask spatial filter in the focal plane of the cylindrical lens "codes" the deflection function "h" (Fig. 24) onto it. The deflection function then appears as a shadow boundary. In the form shown in Fig. 25 some axial uniformity of the preform is assumed. The method by which the mask codes the deflection function onto the x axis is as follows. If the deflection function "h" is negative as shown in Fig. 25, then the ray must be moved down (negative x) in the plane of the mask in order to encounter the mask edge. The shadow therefore moves down in x in the image plane, and conversely up if h is positive.

In the other method, due to Peri, Chu, and Whitbread [58] a similar effect is achieved using an angled slit source and/or an angled cylindrical lens. In this case the deflection function appears as a bright line rather than a shadow boundary.

As measurement techniques, both of the above methods have the disadvantage that the required information appears in a two-dimensional display that must be scanned in both dimensions in order to analyze it.

The Spatial Filtering Technique: An alternative version of the spatial filtering approach that requires imaging in only one dimension was devised by Sasaki, Payne, and Adams [62]. In this method (see Fig. 26) a spherical rather than a cylindrical lens is used, although this is not crucial. The important

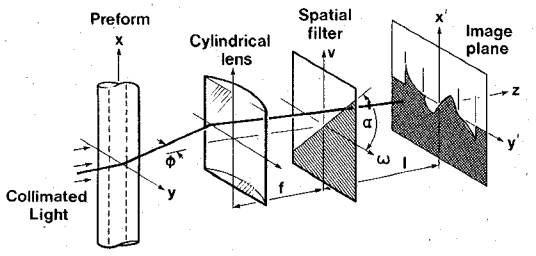

Fig. 25. The apparatus used by Sasaki, Payne, and Adams in the spatial filtering method [60].

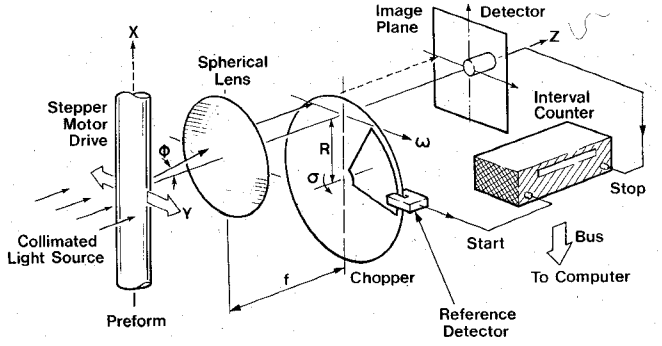

Fig. 26. Apparatus used by Sasaki, Payne, Mansfield, and Adams for time-encoded spatial filtering [62].

difference is that the fixed angled spatial filter is replaced by a vertical one moving along the y axis. Different values of "h" are therefore encoded according to the time at which the edge of the filter reaches that value of h. In the plane where the preform is imaged this information can be extracted using a time-measuring detection system and an appropriate reference. The detector need now only be scanned in one plane (y). This is electronically much more convenient and there are fewer restrictions on axial uniformity. The method can therefore be used to extract axial variation information. Resolution has been shown to be ~16 μm. The method is probably applicable only to preforms. An incoherent light source is used.

The Focusing Method: This method also only requires a scan in the y direction but the "encoding" used is of light intensity and is achieved without special optics. Consider again Fig. 24. If the ray illustrated does not cross any of the rays incident at $y < y_o$, it is evident that these must be bunched together in the region $y < h$ in the observation plane, and that the light intensity in this region is therefore higher than it would have been in the absence of the preform (or fiber). More generally, if two closely spaced rays are separated by δy at the input and δh in the observation plane, then the light intensity will be decreased or increased according to whether $\delta h/\delta y$ is greater or less than one. A measurement of light intensity as a function of y can therefore be used to find dh/dy as a function of y and so the deflection function $h(y)$. The measured distribution will also, of course, depend upon x (Fig. 24).

This method is due to Marcuse [63] and he has shown that the deflection function is obtained from the light intensity distribution $P(h)$ using the relation

$$y_o - h_o = \int_0^{h_o} \left(\frac{P(h)}{P} - 1 \right) dh \qquad (16)$$

where h_o corresponds to y_o for a given ray and P is the (uniform) incident light intensity. The quantity on the left of (16) becomes the required deflection function if divided by x.

This method has been used with both fibers and preforms. Resolution in the former case is comparable with axial interferometry and the method is more widely used with preforms. The method can be very accurate, but has two possible disadvantages. First, because the information is encoded as a variable intensity great care must be taken to ensure uniformity and cleanliness of the source, optics, and detector. Second, the equation (16) implicitly assumes that rays do not cross one another between object and observation planes. This is ensured by keeping x short, but of course, x must exceed the core radius. In theory this is not necessarily sufficient, but it does not usually cause problems. It may be a problem with "W" fibers, however [59].

The extra computation requires care to avoid systematic errors from creeping in. In practice the observation plane is not observed directly, but is enlarged optically to ease measurement, and measurement is automated [64].

Shearing Interferometry: The required deflection function $d\psi/dy$ can be obtained directly by the technique of shearing interferometry. In this method the wavefront emerging from the fiber is divided and one part is displaced by a small amount in the y direction. When the two parts are recombined the resulting fringes show the phase difference $\delta\psi$ for the small shift δy and, thus, read direct in $d\psi/dy$. The apparatus used is shown in Fig. 27. This method can be used with preforms in spite of the difficulties encountered with two-beam transverse interferometry because the phase shift, and therefore, the number of fringes, can be reduced to a manageable level by reducing the shearing shift δy. The method has been used for both fibers and preforms by Kokubun and Iga and others [67]-[69], but is perhaps most useful for preforms. An equivalent technique using holography was used by Chu and Peri [70].

The method is accurate but does, in common with other interference methods, require fairly complex apparatus.

Tomographic Analysis: Although preforms (or fibers) of elliptical cross section may be accommodated by an adaption of the usual deflection function analysis method [54], [71], more complex cross sections require analysis by tomographic techniques. These use a computer and the analysis is relatively complex and time consuming. It is not appropriate to consider the computational problem here. This approach avoids the errors due to slight irregularities of cross section that may otherwise limit the accuracy of the transverse approach. Tomographic analysis has been performed by a number of authors on data obtained in several different ways [72]-[77].

One important point should be made however. The information required for the tomographic analysis is obtained by rotating the preform so that deflection function information is obtained at a number of different azimuths. This may be regarded as measuring points along a series of rotated diameters. It can therefore be seen that the effective spatial density of measurements decreases away from the center of rotation, normally the preform axis. If an insufficient number of azimuths is used, the reconstruction will contain systematic errors that appear as ripples with some symmetry, the ampli-

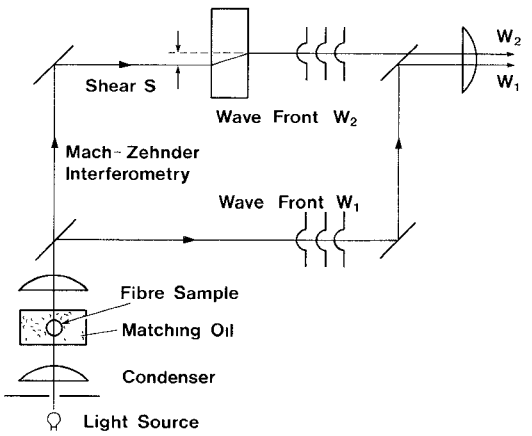

Fig. 27. Apparatus used for transverse shearing interferometry. From Kokubun and Iga [65].

tude of which increases with distance from the axis. It has been shown by Francois, Sasaki, and Adams [76] that the number of azimuths may need to exceed 100 if resolution is not to be lost. This is not very practical and the ripples mentioned show in the results of most authors. However, by taking advantage of the remaining symmetry of the preform the authors in [76] devised an interpolation technique to increase the density of "points" away from the axis. They were then able to reduce the number of azimuths required to 3 for most cases, considerably increasing the attractiveness of tomography. Even so, a significant increase in computing time is required compared with the circular symmetric analysis.

Nonrefractive and Nonoptical Methods: A number of profiling methods have been used that measure composition rather than refractive index. All are open to the objection, at least in principle, that the quantity measured may not be proportional to refractive index. This may be especially true if multiple dopants are involved.

It is possible to use the electron microprobe instrument to examine the ends of fibers and preforms. This uses electron induced X-ray emission to produce composition profiles. Noise-limited sensitivity may be indifferent with some dopants and the resolution is disappointingly poor (>2 μm) because of electrons spreading beneath the surface. It is, however, possible to distinguish different dopants.

It is also possible by careful choice of wavelength to profile preforms using X-ray absorption [78], [79]. Inversion is by the use of an Abel transform. Accuracy may not be very high but, in principle, different dopants might be distinguished.

Fluorescence in preforms excited by ultraviolet radiation may be used to distinguish profiles [80]-[82]. If a thin He-Cd laser beam is used along a diameter, mathematical inversion may be unnecessary, the profile appearing directly as a brightness distribution. There may be some doubt, however, as to the relationship between dopant concentration and fluorescence brightness.

Conclusions

It is very difficult to make meaningful comparisons between different methods, more so because relatively few comparative surveys have been performed [83]-[85]. Those there are, on fibers, suggest that most methods can achieve high accuracy if carefully performed. Resolution considerations probably favor RNF and this may be decisive for monomode fibers. Simplicity of apparatus probably favors near-field methods generally, and BNF is widely used for dimensional measurements mainly for this reason.

Preform profiling is even harder to assess beyond the clear preference for deflection function methods. Methods using spatial filtering or focusing seem to be most popular. Any axial method is less likely to be favored for preforms because of its destructive nature, but perhaps more likely to be favored for fibers, this because of the relative ease with which most axial methods cope with departures from circular symmetry. Any method that is restricted to certain classes of fiber, for example, the far-field methods, is less likely to be widely popular. Conversely, no great advantage is gained from applicability to fibers and preforms because the apparatus used would not normally be compatible with both. The choice of a method must ultimately depend upon many such considerations according to individual requirements.

Acknowledgment

The author is especially grateful to those who sent him prepublication copies of their work for inclusion in this review.

References

[1] R. Olshansky and S. M. Oaks, "Differential mode delay measurement," presented at the 4th European Opt. Commun. Conf., Genoa, Sept. 1978.

[2] F.M.E. Sladen, D. N. Payne, and M. J. Adams, "Definitive profile-dispersion data for germania-doped silica fibres over an extended wavelength range," *Electron. Lett.*, vol. 15, p. 469, 1979.

[3] ——, "Measurement of profile dispersion in optical fibres: A direct technique," *Electron. Lett.*, vol. 13, p. 212, 1979.

[4] D. Gloge, I. P. Kaminow, and H. M. Presby, "Profile dispersion in multimode fibres: Measurement and analysis," *Electron. Lett.*, vol. 11, pp. 469-471, 1975.

[5] W. Eickhoff and E. Wiedel, "Measuring method for the refractive index profile of optical glass fibres," *Opt. and Quantum Electron.*, vol. 7, no. 2, pp. 109-113, 1975.

[6] M. Ikeda, M. Tateda, and H. Yoshikiyo, "Refractive index profile of a graded index fiber, measurement by a reflection method," *Appl. Opt.*, vol. 14, no. 4, pp. 814-815, 1975.

[7] M. Tateda, "Single-mode-fiber refractive-index profile measurement by reflection method," *Appl. Opt.*, vol. 17, no. 3, pp. 475-478, 1978.

[8] T. Wilson, J. N. Gannaway, and C.J.R. Sheppard, "Optical fibre profiling using a scanning optical microscope," *Opt. and Quantum Electron.*, vol. 12, no. 4, pp. 341-345, 1980.

[9] M. Calzavara, B. Costa, and B. Sordo, "Stability and noise improvement in reflectometric index measurement," presented at the Symp. Opt. Fibre Measurements, Boulder, CO, 1980.

[10] J. Stone and H. E. Earl, "Surface effects and reflection refractometry of optical fibres," *Opt. and Quantum Electron.*, vol. 8, no. 5, pp. 459-463, 1976.

[11] C.J.R. Sheppard and A. Choudhury, "Image formation in the scanning microscope," *Opt. Acta*, vol. 24, p. 1051, 1977.

[12] I. Sasaki, D. N. Payne, and R. J. Mansfield, "Direct viewing and measurement of two-dimensional refractive index profiles in optical fibre preforms," presented at OFC '82, Phoenix, AZ, Apr. 1982.

[13] F.M.E. Sladen, D. N. Payne, and M. J. Adams, "Determination of optical fiber refractive index profiles by a near-field scanning technique," *Appl. Phys. Lett.*, vol. 28, no. 5, pp. 255-258, 1976.

[14] W. J. Stewart, "A new technique for measuring the refractive index profiles of graded optical fibres," in *Proc. IOOC*, Tokyo, Japan, 1977, paper C2-2.

[15] K. I. White, "Practical application of the refracted near-field technique for the measurement of optical fibre refractive index profiles," *Opt. and Quantum Electron.*, vol. 11, no. 2, pp. 185-196, 1979.

[16] W. J. Stewart, *Scanning Microscopy*, E. Ash, Ed. New York: Academic, 1981.
[17] J. A. Arnaud and R. M. Derosier, "Novel technique for measuring the index profile of optical fibers," *Bell Syst. Tech. J.*, vol. 55, no. 10, pp. 1489–1508, 1976.
[18] M. J. Adams, D. N. Payne, F.M.E. Sladen, and A. Hartog, "Resolution limit of near field scanning technique," presented at the 3rd ECOC, Munich, Germany, 1977.
[19] J. P. Hazan, "Intensity profile distortion due to resolution limitation in fibre index profile determination by near field," *Electron. Lett.*, vol. 14, p. 158, 1978.
[20] A. W. Snyder and C. Pask, "Optical fibre: Spatial transient and steady state," *Opt. Commun.*, vol. 15, p. 314, 1975.
[21] M. J. Adams, D. N. Payne, and F.M.E. Sladen, "Correction factors for the determination of optical-fibre refractive index profiles by the near field scanning technique," *Electron. Lett.*, vol. 12, p. 281, 1976.
[22] K. Petermann, "Leaky mode behaviour of optical fibres with non-circularly symmetric refractive index profile," *Arch. Elek. Übertragung*, vol. 31, p. 201, 1977.
[23] P.V.H. Sabine, F. Donaghy, and D. Irving, "Fibre refractive-index profiling by modified near-field scanning," *Electron. Lett.*, vol. 16, no. 23, pp. 882–883, 1980.
[24] M. J. Saunders, "Optical fiber profiles using the refracted near-field technique. A comparison with other methods," *Appl. Opt.*, vol. 20, no. 9, pp. 1645–1651, 1981.
[25] M. Young, "Calibration technique for refracted near-field scanning of optical fibers," *Appl. Opt.*, vol. 19, no. 15, pp. 2479–2480, 1980.
[26] D.C.J. Reid and W. J. Stewart, "Ultrahigh resolution refractive near field profiling," in *Proc. IOOC '81*, San Francisco, CA, paper TuG6.
[27] T. Okoshi and Y. Era, "Measurement of two-dimensional refractive-index distribution in a preform using a modified Stewart's method," to be published.
[28] G. K. Grau and O. G. Leminger, "Relations between near field and far field intensities, radiance and modal power distribution of multimode graded index fibres," *Appl. Opt.*, vol. 20, p. 457, 1981.
[29] W. Freude, "Far-field profiling of multimode optical fibres," *Electron. Lett.*, vol. 17, no. 11, pp. 385–387, 1981.
[30] K. Hotate and T. Okoshi, "Measurement of refractive-index profile and transmission characteristics of a single-mode optical fiber from its exit-radiation pattern," *Appl. Opt.*, vol. 18, no. 19, pp. 3265–3271, 1979.
[31] W. A. Gambling, D. N. Payne, H. Matsumura, and R. B. Dyott, "Determination of core diameter and refractive index difference of single-mode fibres by observation of the far-field patterns," *Microwaves Opt. and Acoust.*, vol. 1, no. 13, 1976.
[32] W. E. Martin, "Refractive index profile measurements of diffused optical waveguides," *Appl. Opt.*, vol. 13, no. 9, pp. 2112–2116, 1974.
[33] J. Stone and R. M. Derosier, "Elimination of errors due to sample polishing in refractive index profile measurements by interferometry," *Rev. Sci. Instru.*, vol. 47, no. 7, pp. 885–887, 1976.
[34] H. M. Presby and H. W. Astle, "Optical fiber index profiling by video analysis of interference fringes," *Rev. Sci. Instru.*, vol. 49, no. 3, pp. 339–344, 1978.
[35] J. Stone and H. E. Earl, "Optical fiber refractometry by interference microscopy: A simplified method," *Appl. Opt.*, vol. 17, pp. 3647–3652, 1978.
[36] Y. Kokubun and K. Iga, "Index profiling of distributed index lenses by a shearing interference method," *Appl. Opt.*, vol. 21, no. 6, pp. 1030–1034, Mar. 1982.
[37] D. Marcuse, *Principles of Optical Fibre Measurement*. New York: Academic, 1981.
[38] T. Okoshi and M. Nishimura, "Automated measurement of refractive index profile of VAD preforms by fringe-counting method," *J. Opt. Commun.*, vol. 1, p. 18, 1980.
[39] M. J. Saunders and E. D. Head, "Small scale core fluctuations in multimode MCVD fibres," in *Proc. IOOC '81*, San Francisco, CA, paper TUG4.
[40] A. M. Hunter and D. W. Schreiber, "Mach–Zehnder interferometer data reduction method for refractively inhomogeneous test objects," *Appl. Opt.*, vol. 14, p. 634, 1975.
[41] M. E. Marhic, P. S. Ho, and M. Epstein, "Nondestructive refractive-index profile measurements of clad optical fibers," *Appl. Phys. Lett.*, vol. 26, no. 10, pp. 574–575, 1975.
[42] K. Iga and Y. Kokubun, "Precise measurement of the refractive index profile of optical fibres by a nondestructive interference method," in *Proc. IOOC*, Tokyo, Japan, 1979, p. 399.
[43] M. J. Saunders and W. B. Gardner, "Nondestructive interferometric measurement of the delta and alpha of clad optical fibers," *Appl. Opt.*, vol. 16, no. 9, pp. 2368–2371, 1977.
[44] K. Iga and Y. Kokubun, "Formulas for calculating the refractive index profile of optical fibers from their transverse interference patterns," *Appl. Opt.*, vol. 17, no. 12, pp. 1972–1974, 1978.
[45] H. M. Presby, D. Marcuse, and L. M. Boggs, "Rapid and accurate automatic index profiling of optical fibres," in *Proc. ECOC*, Genoa, 1978, p. 162.
[46] P. L. Chu and T. Whitbread, "Nondestructive determination of refractive index profile of an optical fiber: Fast Fourier transform method," *Appl. Opt.*, vol. 18, no. 7, pp. 1117–1122, 1979.
[47] D. Marcuse and H. M. Presby, "Light scattering from optical fibres with arbitrary refractive index distribution," *J. Opt. Soc. Amer.*, vol. 65, p. 361, 1975.
[48] T. Okoshi and K. Hotate, "Refractive-index profile of an optical fiber: Its measurement by the scattering-pattern method," *Appl. Opt.*, vol. 15, no. 11, pp. 2756–2764, 1976.
[49] K. Hotate and T. Okoshi, "Semiautomated measurement of refractive index profiles of single mode fibres by the scattering-pattern method," in *Proc. IOOC*, Tokyo, Japan, 1977, paper C2.3.
[50] C. Saekeang and P. L. Chu, "Nondestructive determination of refractive-index profile of an optical fibre: Forward light scattering method," *Electron. Lett.*, vol. 14, no. 25, pp. 802–804, 1978.
[51] E. Brinkmeyer, "Refractive-index profile determination of optical fibers from the diffraction pattern," *Appl. Opt.*, vol. 16, no. 11, pp. 2802–2803, 1977.
[52] ——, "Refractive-index profile determination of optical fibers by spatial filtering," *Appl. Opt.*, vol. 17, no. 1, pp. 14–15, 1978.
[53] P. L. Chu, "Nondestructive measurement of index profile of an optical-fibre preform," *Electron. Lett.*, vol. 13, no. 24, pp. 736–738, 1977.
[54] K. F. Barrell and C. Pask, "Nondestructive index profile measurement of noncircular optical fibre preforms," *Opt. Commun.*, vol. 27, no. 2, pp. 230–234, 1978.
[55] P. L. Chu and T. Whitbread, "Measurement of refractive-index profile of optical-fibre preform," *Electron. Lett.*, vol. 15, no. 10, pp. 295–296, 1979.
[56] L. S. Watkins, "Laser beam refraction traversely through a graded-index preform to determine refractive index ratio and gradient profile," *Appl. Opt.*, vol. 18, no. 13, pp. 2014–2222, 1979.
[57] I. Sasaki and D. N. Payne, "Simple visual inspection technique for optical fibre preforms," *Electron. Lett.*, vol. 17, p. 805, 1981.
[58] T. Okoshi and M. Nishimura, "Measurement of axially nonsymmetrical refractive-index distributions of optical fiber preforms by a triangular mask method," *Appl. Opt.*, vol. 20, no. 14, pp. 2407–2411, 1981.
[59] D. Peri, P. L. Chu, and T. Whitbread, "Direct display of deflection function of optical fibre preforms," *Appl. Opt.*, vol. 21, no. 5, pp. 809–814, Mar. 1982.
[60] I. Sasaki, D. N. Payne, and M. J. Adams, "Measurement of refractive-index profiles in optical-fibre preforms by spatial-filtering technique," *Electron. Lett.*, vol. 16, no. 6, pp. 219–221, 1980.
[61] I. Sasaki, P. L. Francois, and D. N. Payne, "Accuracy and resolution of preform index profiling by the spatial-filtering method," in *Proc. ECOC7*, Copenhagen, Denmark, 1981, paper 6.4.
[62] I. Sasaki, D. N. Payne, R. J. Mansfield, and M. J. Adams, "Variation of refractive-index profiles in single-mode fibre preforms measured using an improved high-resolution spatial-filtering technique," in *Proc. 6th European Conf. on Opt. Commun.*, York, England, Sept. 1980, pp. 140–143.
[63] D. Marcuse, "Refractive index determination by the focusing method," *Appl. Opt.*, vol. 18, no. 1, pp. 9–13, 1979.
[64] H. M. Presby and D. Marcuse, "Preform index profiling (PIP)," *Appl. Opt.*, vol. 18, no. 5, pp. 671–677, 1979.
[65] Y. Kokubun and K. Iga, "Precise measurement of the refractive index profile of optical fibers by a non-destructive interference method," *Trans. Inst. Electron. Commun. Eng. Japan*, vol. E60, no. 12, pp. 702–707, 1977.
[66] H. M. Presby, D. Marcuse, and W. G. French, "Refractive-index profiling of single-mode optical fibers and preforms," *Appl. Opt.*, vol. 18, no. 23, pp. 4006–4011, 1979.

[67] Y. Ohtsuka and Y. Shimizu, "Radial distribution of the refractive index in light-focussing rods: Determination using Interphako interference microscopy," *Appl. Opt.*, vol. 16, p. 1050, 1979.
[68] Y. Kokubun and K. Iga, "Refractive-index profile measurement of preform rods by a transverse differential interferogram," *Appl. Opt.*, vol. 19, no. 6, pp. 846–851, 1980.
[69] Y. Ohtsuka and Y. Koike, "Determination of the refractive-index profile of light-focussing rods: Accuracy of a method using Interphako interference microscopy," *Appl. Opt.*, vol. 19, p. 2866, 1980.
[70] P. L. Chu and D. Peri, "Holographic measurement of refractive-index profile in the transition region of an optical fiber preform," *Appl. Opt.*, vol. 20, no. 8, pp. 1418–1423, 1981.
[71] P. L. Chu, "Non-destructive refractive-index profile measurement of elliptical optical fibre or preform," *Electron. Lett.*, vol. 15, no. 12, pp. 357–358, 1979.
[72] P. L. Chu and C. Saekeang, "Non-destructive determination of refractive-index profile an cross-sectional geometry of optical-fibre preform," *Electron. Lett.*, vol. 15, no. 20, pp. 635–637, 1979.
[73] C. Seakeang, P. L. Chu, and T. W. Whitbread, "Non-destructive measurement of refractive-index profile and cross-sectional geometry of optical fiber preforms," *Appl. Opt.*, vol. 19, no. 12, pp. 2025–2030, 1980.
[74] T. L. Francois, T. Sasaki, and M. J. Adams, "Three-dimensional fibre preform profiling," *Electron. Lett.*, vol. 17, p. 876, 1981.
[75] T. Okoshi and M. Nishimura, "Measurement of axially non-symmetrical refractive-index distributions of optical fibre preforms by a triangular mask method," *Appl. Opt.*, vol. 20, p. 2047, 1981.
[76] P. Francois, I. Sasaki, and M. J. Adams, "Practical 3-D profiling of optical fiber performs," *IEEE J. Quantum Electron.*, vol. QE-18, pp. 524–535, Apr. 1982.
[77] T. Okoshi and M. Nishimura, "Measurement of axially non-symmetrical refractive index distribution of single-mode fibre by a multidirectional scattering-pattern method," to be published.
[78] H. Takahashi, K. Nakamura, S. Shibuya, and T. Kuroha, "Inspection method of optical fiber preforms by X-ray absorption measurements," *Furukawa Electron. Rev.* (Japan), vol. 68, pp. 143–149, 1980.
[79] S. Tanaka, G. Tanaka, M. Hoshikawa, and N. Inagaki, "Non-destructive refractive index profile determination of optical fibre preform using X-rays," in *Proc. ECOC6*, York, England, Sept. 1980, p. 165.
[80] H. M. Presby, "Fluorescence profiling of single-mode optical fiber preforms," *Appl. Opt.*, vol. 20, no. 3, pp. 446–450, 1981.
[81] —, "Ultraviolet-excited fluorescence in optical fibers and preforms," *Appl. Opt.*, vol. 20, no. 4, pp. 701–706, 1981.
[82] H. M. Presby and D. Marcuse, "Preform core diameter measurement by fluorescence," *Appl. Opt.*, vol. 20, p. 4324, 1981.
[83] H. M. Presby, "Profile characterisation of optical fibres–A comparative survey," *Bell Syst. Tech. J.*, vol. 60, p. 1335, 1981.
[84] B. Costa and B. Sordo, "Measurements of the refractive index profile of optical fibres: Comparison between different techniques," in *Proc. ECOC2*, Paris, France, Sept. 1976, p. 81.
[85] M. J. Saunders, "Optical fibre profiles using the refracted near field technique, a comparison with interferometry," presented at the Meet. on Optical Fibre Measurements, Boulder, CO, 1980.
[86] D. Marcuse and H. M. Presby, "Index profile measurements of fibres and their evaluation," *Proc. IEEE*, vol. 68, no. 6, pp. 666–688, 1980.

W. J. Stewart received the Bachelor's degree (Honors) in physics, in 1968, and the Msc. degree with distinction in optics from London University, London, England, where he continued Postgraduate work until 1971.

In 1971 he joined the Allen Clark Research Centre, Plessey Research (Caswell) Limited, Caswell, Towcester, Northants., England, where his primary areas of work have been in the optics of fibers for communication, mainly on various aspects of measurement and propagation. He has also worked on optical couplers and connectors. He has participated in the international workshops on optical fiber theory. Recently, he has worked on integrated optics and display optics and is currently Group Leader on all optical work at Caswell, including fiber optics.

Dr. Stewart is a member of EPS, IOP, and the Optical Society of America.